Assembly and characterization of ZnO nanoparticles for Grätzel's solar cells

Glécia V. S. Luz[1,2*], Wang. S. Hui[1], Renata C. Roncoleta[2], Pedro H. O. Nogueira[2], Lourdes M. Brasil[2], Pilar Hidalgo[2*]

[1]*Departamento de Metalurgia e Materiais, Escola Politécnica da USP, University of São Paulo-USP, Av. Prof. Mello Moraes 2463, São Paulo-SP, 05508-030, Brazil*
[2]*UnB at Gama-FGA, University of Brasília-UnB, Área Especial de Indústria Projeção A, Brasília-DF, 72444-240, Brazil*

*Corresponding authors

Abstract

This research aimed to build hybrid solar cells, based on Grätzel method. We used the Polyethylene Terephthalate (PET) polymer as a substrate containing a layer of Indium Tin Oxide (ITO). Films of ZnO nanoparticles (ZnO NPs) synthesized by Pechini Method, and four different dyes were tested: Congo Red (CR), Bromocresol Green (BG), Acridine Orange (AO) and a Ruthenium Complex (RC). ZnO NPs were analyzed by XRD, which generated peaks corresponding to hexagonal wurtzite crystalline structure. We also conducted analysis by UV–Vis. Spectroscopy and Transmission Electron Microscope (TEM). Rietveld analysis determined the crystal size of 115.23 ± 28.16 nm. The deposition of ZnO and dye thin films were made through spin-coating. The electrical properties of the formed films were characterized with Van der Pawn method. Efficiency in converting light in electricity under an OSRAM 20W light bulb was tested after the devices were built. The smaller sheet resistance results were obtained for material containing: PET/ITO/ZnO/CR and PET/ITO/ZnO/AO. As expected, the best open-circuit voltage (V_{oc}) results reached were 64 and 73 mV to CR and AO, respectively. Therefore, the results demonstrated satisfactory interaction between the ZnO-Dye-Electrolyte layers. Copyright © 2018 VBRI Press.

Keywords: ZnO, nanoparticles, Grätzel's solar cell, PET, dye-sensitized solar cell.

Introduction

The research of renewable energy has been growing in recent decades with the prospects of being power sources that can provide light, electricity and heat without polluting the environment. It is known that one of the biggest causes of environment pollution is the use of fossil fuels. Another drawback of fossil fuels is its finite obtainability. Examples of alternative sources of renewable energy include solar, hydropower, wind, biomass, hydrogen and geothermal energies. At present, there is a large interest in this area since it is expected to supply 50% of the world's primary energy by 2040. Moreover, these clean energies are able to reduce gas emissions to the environment by about 70% in 2050 [1].

Solar photovoltaic (PV) can fulfill this role as Earth receives more solar energy in an hour than we consume in an entire year. For example, if we cover 0.16% of the earth's surface with solar cells with a 10% efficiency rate we would have the capacity to generate electricity more than enough to supply all countries [2].

The photovoltaic cell was first proposed as a power generator device by Chapin, Fuller and Pearson in 1954 using a silicon p-n junction, with 6% efficiency. After several efficiency studies regarding the device crystalline silicon structure, it reached 24% of efficiency, currently dominating the solar cell market [3,4]. Some of the best organic photovoltaic cells have 5% efficiency and semiconducting polymers are prepared with poly(hexylthiophene) and fullerene derivatives.

There are several types of materials that can make PVs. According to the material involved, PV may be divided into [1,5,6]: i) Dye-sensitized solar cell (DSSC); ii) Organic-polymer-based PV solar cell (OPV) and iii) Hot carrier solar cells. This work was carried out using DSSC's specifically. This kind of solar cell enables optical absorption by associating a dye sensitizer (that absorbs the light) with a nanometric semiconductor as the photoanode. It is based on semiconductor framework with electrolytes (e.g. iodine, in this case) as substitute to the p–n junctions of inorganic solid-state semiconductors in traditional solar cells.

The inception of research on polymers as the active layer in solar cells date back from the 90s, and in 2010 researches obtained a 7.4% efficiency [7,8]. Often, Tin Oxide (TO) films with Fluorine Tin Oxide (FTO) doping or Indium Tin Oxide (ITO) are used. The second electrode may be composed of aluminum, calcium, gold, magnesium [9] or graphite.

Nanotechnology is a science field that has grown quickly in the recent years due to many engineering and technological applications[1]. A application example is the construction of PV with nanocrystalline semiconductor oxide film, such as ZnO, NbO_5, SnO_2, Al_2O_3, TiO_2 and zeolite [10]. It was observed that the use of nanocomposites is effective in modifying the

electrical characteristics of devices, improving their performance[**11**]. Zinc Oxide (ZnO) is an inorganic compound extensively used by several products including: lubricants, plastics, glass, rubber, cement, ceramics and photo-eletrovoltaic devices, also with applications in biomedical engineering[**1**,**8**]. Hence, there is a great amount of studies about these semiconductors, surrounding nanometric dimensions and different synthesis methods. ZnO Nanoparticles (NPs) exhibit specific optical, electrical and morphological characteristics compared to molecules of larger dimensions. One of the structural shapes that can be obtained is the cubic rock salt, hexagonal wurtzite or cubic zinc blend. It is an n-type semiconductor transparent in the visible light that absorbs UV light [**10**,**12**].

ZnO NPs can be obtained with different grain sizes depending on the method of synthesis. Some methods used are: electroplating [**13**–**17**], hydrothermal [**18**–**20**], sonochemical [**21**], sol-gel [**22**–**24**], Pechini [**25**–**29**], spray pyrolysis [**3**], wet chemical [**30**] and zinc-air system [**31**]. For this research, the chosen synthesis methodology was the Pechini Method (PM), due to the possibility of producing nanoparticles with good homogeneity, optical and structural characteristic, inexpensive reagents, moderate temperatures and easy process control.

DSSCs usually follows the Grätzel method [**32**] where in one of its layers are sensitized by dyes. The main operating mechanism of solar energy conversion on an DSSCs are: light absorption, charge injection, electron transport and collection, and electrolyte diffusion [**33**]. This work studied DSSCs with different dyes and their interactions with nanoparticles of ZnO, in a PET substrate. Thus verifying the changes in the electron transport between these materials [**33**,**34**]. PVs made with these materials allow the creation of flexible, lighter, cheaper, easier to produce (even from recyclables) and install solar panels. Thus, in view of these facts, the characteristics presented and the interest of the academic community in ZnO NPs, it was decided to use it in the studies of the proposed DSSCs.

Thus, this research aimed to synthesize hybrid solar cells - based on Grätzel method - using PET substrate and ITO layers. Films of ZnO NPs, and four different kinds of sensitizing dyes were tested, namely: Congo Red (CR), Bromocresol Green (BG), Acridine Orange (AO) and Ruthenium Complex (RC) (cis-bis (isothiocyanato) bis (2, 21'-bipyridyl-4,4'-dicarboxylato) ruthenium (III)). The films produced were characterized with respect to electrical properties. The conversion efficiency of the devices was tested using an OSRAM 20W light bulb.
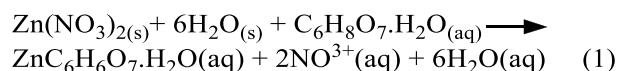
Experimental

Materials

ZnO NPs were prepared via Pechini Method [**28**]. While, Zinc Nitrate ($ZnC_6H_6O_7.H_2O$), Ethylene Glycol monohydrate P.A. (EG) ($C_2H_6O_2.H_2O$), Ethyl Alcohol P.A. (CH_3CHOH), Citric Acid monohydrate (CA) ($C_6H_8O_7.H_2O$) were purchased from Vetec company. The substrate of PET+ITO were acquired by Sigma-Aldrich Company, and have sheet resistance in the order of 60 Ω/sheet. The dyes used were: Congo Red (CR) ($C_{32}H_{22}N_6Na_2O_6S_2$), Bromocresol Green (BG) ($C_{21}H_{14}Br_4O_5S$) 95%, Acridine Orange Solution (AO) - 2% in H_2O - and Ruthenium Complex (RC) (cis-bis (isothiocyanato) bis (4-2,21'-bipyridyl, 4'-dicarboxylato) ruthenium (III)) 95%, were also supplied by Sigma-Aldrich Company. An OSRAM DULUX® electronic energy-saving lamp 20W 220V was used for the tests. Also, the Iodine ($\geq$ 99,8%) was purchased from Sigma-Aldrich Company.

Synthesis of ZnO Nanoparticles by Pechini Method

Owing to its photoelectric properties, piezoelectric and chemical stability, the ZnO was used in this study for the assembly of photovoltaic cells. According to Rasavi et al. (2012) [**28**], the steps followed for the synthesis were: Chelate-forming cations, polyesterification and ZnO formation. The first step, chelate-forming cations (Zn^{2+}) use 5.00±0.01 g of Zinc Nitrate solubilized in 15.00±0.03 mL deionized water, with 5.02±0.01 g of Citric Acid monohydrate. The reaction is described in Equation (**1**):

$$Zn(NO_3)_{2(s)} + 6H_2O_{(s)} + C_6H_8O_7.H_2O_{(aq)} \longrightarrow$$
$$ZnC_6H_6O_7.H_2O(aq) + 2NO^{3+}(aq) + 6H_2O(aq) \quad (1)$$

A polymerization reaction, also known as polyesterification, occurs at the second step (**Eq. 2**). The mixture obtained in the first step was added in EG P.A. at 52°C, with (EG:CA) mole ratio 2:1 m/m. This solution was maintained under heating at 50 °C and constant stirring for 1 h.

$$ZnC_6H_6O_7.H_2O_{(aq)} + C_2H_6O_2.H_2O_{(aq)} \longrightarrow$$
$$ZnC_8H_{10}O_8.H_2O_{(aq)} + H_2O_{(aq)} \quad (2)$$
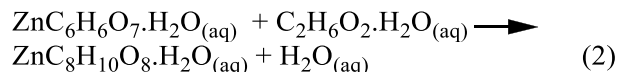
In the final step, the solution was heated following temperatures ramps of 30-80-150-600°C with 10°/min as heating rate. When temperatures of 80, 150 and 600°C were reached, an interval of 1 hour was taken until the next ramp heating. Accordingly, after reaching the temperature of 600°C and maintaining this temperature for one hour, the muffle was turned off and the temperature was decreased until room temperature. The goal of this procedure is to eliminate the organic component, to obtain pure ZnO NPs [**26**,**27**].

According to studies, the calcination temperature is the factor that affects most the crystallites size. However, EG and CA proportions also influences the formation of nanoparticles, which is justified by the theory of collisions and Le Chatelier's principle [**9**,**11**].

Characterizations of ZnO Nanoparticles

For NPs characterization and purity analysis of the product obtained, XRD patterns were analyzed on a Bruker D8-Discover diffractometer, with Cu Kα radiation. The angle (2θ) range was 20º-90ºand a continuous scan of 0.020º/min was used. To determine the size of ZnO NPs, Rietveld analyses measurements were performed with a scan step mode of 2θ variation from 20.00º to 89.98º and 0.020º/min of scanning velocity. Analyses were performed in UV–Vis. spectroscopy for studies about optical absorbance with an Evolution 220 Thermo Scientific spectrometer. Dimensional and morphological analyses were also performed using a Transmission Electron Microscope (TEM), JEOL, JEM-1011 model, operated at acceleration voltage of 80.0kV. All measurements were carried out at room temperature.

Assembly and characterization of ZnO Grätzel's Solar Cells

The basic structure of the assembled photovoltaic cell [**32**] contains Transparent Conductive Oxide (TCO), where ZnO NPs are dispersed in ethyl alcohol (CH_3CHOH), that functions as a carrier of electrons and holes. The material was deposited on a PET substrate, which already contained a thin layer of Indium Tin Oxide (ITO) on one of its faces. The PET+ITO substrate has dimensions of 2.5x2.5cm.

Immediately above the nanoparticles, a thin layer of dye was deposited. Four different types of dyes were tested: Congo Red (CR), Bromocresol Green (BG), Acridine Orange (AO) and Ruthenium Complex (RC) (cis-bis (isothiocyanato) bis (4-2,21'-bipyridyl, 4'-dicarboxylato) ruthenium (III)). The dyes were diluted in ethyl alcohol and the final concentration of the solutions was 5 mg/ml. Deposition of ZnO NPs and the dyes were performed by a spin-coating constructed with recycled material [**35,36**]. The deposition speed was 3146 rpm and 56.11 ± 0.18s (Position 3). 10 minutes after the deposition, a sheet resistance analysis (Ω/sheet) on Agilent B1500A Semiconductor Device using the Van der Pauw method [**37,38**] was executed. This method provides the film sheet resistance (Ω/area) plot and the voltage variation (DeltaV) generated as a function of electrical current (i) applied to the material.

After deposition of the dye, a thin layer of graphite was deposited on the other cell electrode by mechanical compression. Subsequently, they were assembled together forming the two parts of the cell: Part A (containing PET + ITO + ZnO NPs + Dye) and Part B (PET + ITO + Graphite). The electrolyte between the electrodes consisted of 3 drops of triiodide / iodide (I^-/I_3^-) in acetone, at a concentration of 5 mg/mL. The I^- / I_3^- was used because it is the most common electrolyte used in DSSCs, and according to some authors [**7,8,39**], results in high performance redox couple. The final configuration of the dye sensitized photovoltaic cell is illustrated in **Fig. 1**.
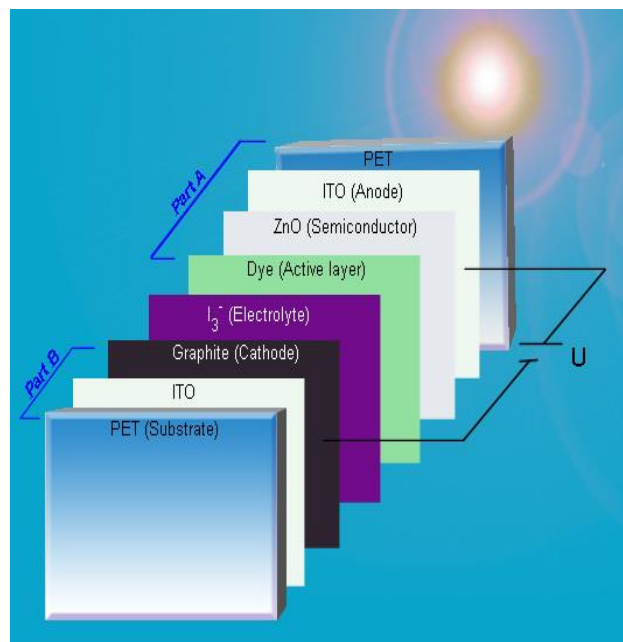

Fig. 1. Basic installation of photovoltaic cells using nanoparticles of ZnO and based on Gratzel method. Where: ITO = indium tin oxide; I_3^- = Electrolyte; PET = polyethylene terephthalate; and U = voltage.

Immediately after assembling the solar cell, its open-circuit voltage (V_{oc}) was obtained under the irradiation of an OSRAM DULUX® electronic energy-saving lamp 20W/220V, two meters away and at a position of 90º. As there was no complete encapsulation of DSSCs, the measurements were performed right after injection of electrolyte, thus preventing its evaporation. The V_{oc} was measured using a multimeter. For each cell, the measurements lasted two minutes and in each, the highest value found during the analysis it the one in use here.

Results and discussion

XRD and Rietveld refinement analyses of ZnO NPs

Fig. 2 shows the XRD patterns and Rietveld refinements analyses of ZnO nanopowders obtained by Pechini method. All diffraction peaks can be indexed as a wurtzite crystalline structure. The results were calculated with structural parameters, as: atomic coordinates, peak shape, cell and width parameters (background, Lorentz-polarization correction, etc.).

The structural parameters were compared with the data obtained (**Table 1**, see Supporting information), between the pattern P6$_3$mc - 186 (Cal.) [**40,41**], based on the hexagonal tetragonal space group, with lattice parameters a=b=3.81 Å and c=6.23 Å and internal coordinates Zn (0.6667; 0.3333; 0.0) and O (0.6667; 0.3333; 0.375) [**42,43**]. The cited data are in agreement with the Joint Committee on Powder Diffraction Standards (JCPDS) card 36-1451.
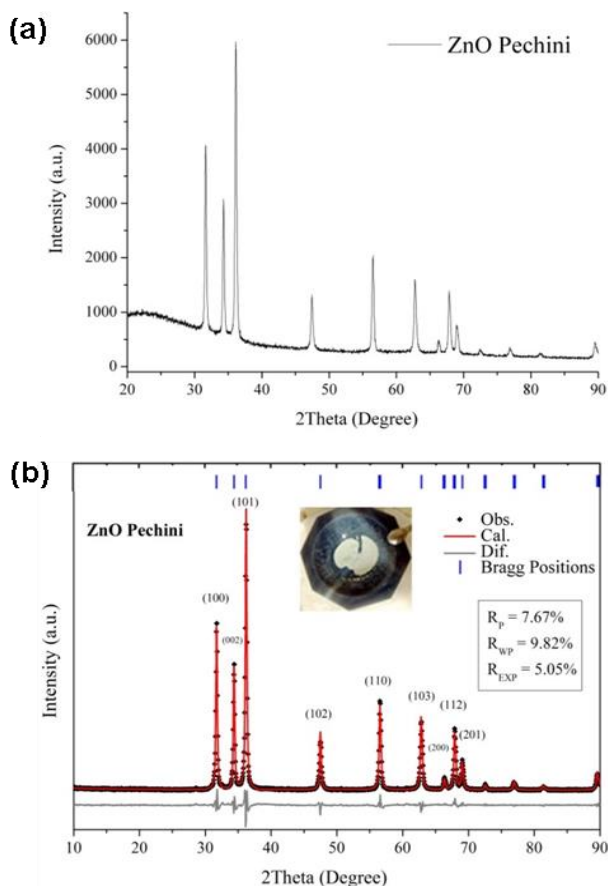
Fig. 2. X-ray Analysis. (a) X-ray diffractogram of ZnO NPs, synthesized with Pechini method; (b) XRD patterns refined with Rietveld method and a picture of the sample. Obs. = the experimental data; Cal. = the theoretical data; Dif. = the difference between patterns. Bragg Position = indicate the peak position; R_{wp} = weighted profile factor; R_p = patterns factor; and R_{exp} = expected weighted profile factor.1

Thus, **Fig. 2b** shows the spectra obtained (Obs.) for the synthesis, and different statistical agreement factors between data: Dif., R_p, R_{wp} e R_{exp}. The R_{wp} factor (weighted profile), R_p (patterns factor) and R_{exp} (expected weighted profile factor). The results not just show how well the structural model fits the measured diffraction intensities, but also show how well we have fit the background and the diffraction positions and peak shapes [**44**,**45**]. **Fig. 2** and **Table 1** (see Supporting information) shows the purity of the hexagonal phase of the wurtzite type of ZnO, which is indicated by the intensity ratio of the peaks demonstrating good crystallinity, specifying that the ZnO NPs obtained by the Pechini method have organized a crystalline structure over long distances or periodically, in order words, completely sorted.

The data indicate that the single phase crystal structure was obtained, and secondary phases are not formed. It is found that the strongest reflections are in the plans (101), (100) and (002), respectively, consistent with the data in the crystallographic form.

The size of the ZnO NPs is modified according to the method, quantity of reagents, temperature and reaction time of the synthesis. The lattice parameters obtained for ZnO NPs is in agreement with the report of literature (JCPDS:89-0510) [**43**], and the volume is proportional to the obtained unit cell parameters. The average crystallite diameter was estimated by the most intense peak (101), according to the diffraction data and Rietveld method and Law Scherrer. This experimental work obtained an average crystallite size of $1.15228 \times 10^{-7} \pm 2.81567 \times 10^{-8}$ m, i.e., 115.23 ± 28.16 nm. The minimum value of crystallite size was 82.21 nm and the maximum was 168.26 nm.

UV–Vis. absorption spectroscopy analysis and determination of band gap energy of ZnO NPs

In **Fig. 3a** we observe the UV–Vis. absorption characteristic of the formed ZnO NPs. It was noted the characteristic wavelength of product. The sample had a broad absorption in the range from 200 to 400 nm. The sample value of the wavelength associated with the transition ZnO NPs (Valence band (BV) - Conduction band (BC)) were observed in 387.72 nm, consistent with those observed in the literature [**46**]. The smaller the radius of the particle size, the greater the wavelength absorbed by the material, shifting the light absorption to smaller wavelength.
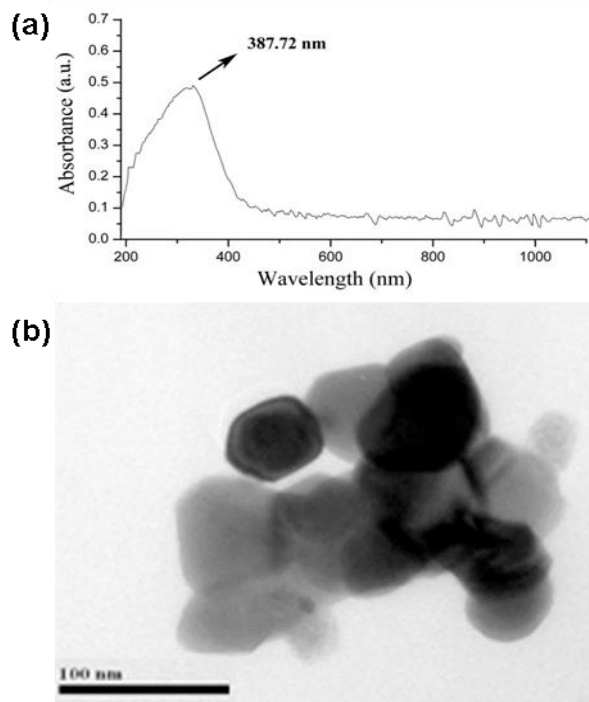

Fig. 3. Results of the ZnO Nanoparticles characterization: (a) UV-Vis. spectra for ZnO NPs synthesized by Pechini Method and (b) TEM image obtained at 80.0kV**.**

The band gap energy (E_g) is a factor of significant importance for characterization of insulator and semiconductor materials. This energy can be characterized by several methods [**47**]. The method used

was the Kubelka and Munk model [**48**]. The E_g value obtained for the ZnO NPs synthesized was 3.39 eV. The results are consistent with literature, that for semiconductors a variation of energy is from 0.2 to 4.0 eV [**46**,**49**,**50**].

TEM results of ZnO NPs

Through the micrography TEM (**Fig. 3b**) the diluted sample (150 ppm) and de-agglomerated ZnO by ultrasonic agitation showed nanoparticles of defined shape and uniform with size crystallite of 50 - 60 nm. The crystalline structure was confirmed as hexagonal wurtzite type tetragonal space group. Furthermore, this equipment allowed the visualization of smaller nanoparticles, when compared to the results of the analysis by X-ray diffraction that showed particle size in the range 115.23 nm- 82.21 nm.

ZnO Grätzel's Solar Cells in PET substrate

Once the making of ZnO NPs was confirmed, we proceeded to the making of DSSCs. **Fig. 4** and **Table 2** show the results obtained for sheet resistance of the ZnO NPs thin films and dyes, after deposition.
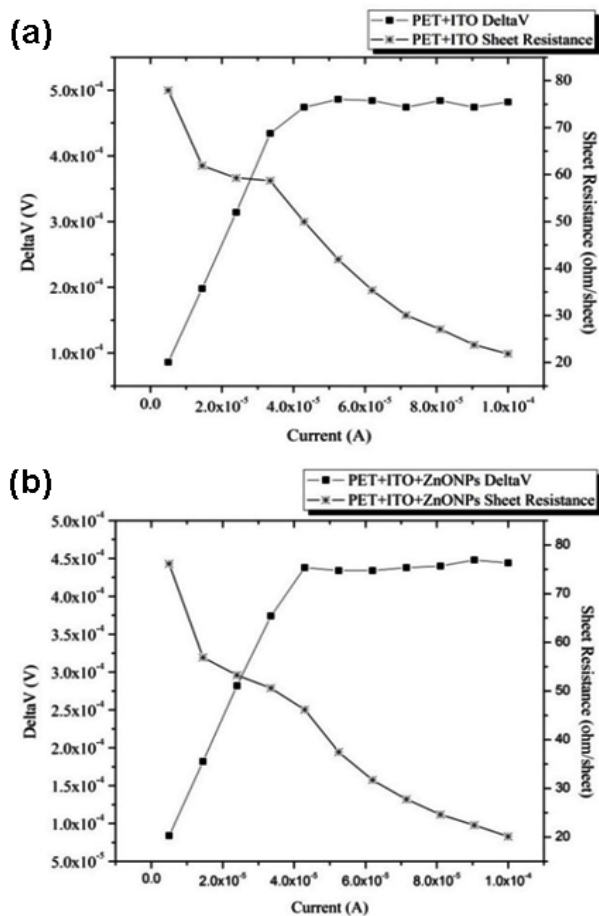

Fig. 4. Results of the electrical characterization of materials, using the technique of the four dots and Van der Pawn method, which shows curves of voltage variation (DeltaV), and sheet resitance (ohm/sheet) in function of the applied current. The materials analyzed here were: (a) PET + ITO and (b) PET + ITO + ZnONPs.

Fig. 4 shows the results of the sheet resistance variation as a function of applied current. When a thin ZnO NPs film was applied on the ITO, there was a slight reduction in sheet resistance. This possibly is related to the characteristic of the semiconductor material used, the ZnO.

Table 2. Results obtained during electrical characterization (Van der Pawn method) of the materials "PET+ITO+ZnONPs" and "PET+ITO+ZnONPs+Dye", i.e., before and after the application of dyes.

Dye	PET+ITO+ZnONPs			PET+ITO+ZnONPs+Dye		
	Current (A)	Delta V (V)	Sheet Resistance (Ω/ sheet)	Current (A)	Delta V (V)	Sheet Resistance (Ω/sheet)
Congo Red	3.35×10^{-4}	4.22×10^{-4}	57.09	3.70×10^{-4}	4.66×10^{-4}	63.05
Acridine Orange	2.60×10^{-4}	4.75×10^{-4}	77.50	3.10×10^{-4}	4.55×10^{-4}	66.52
Ruthenium Complex	2.30×10^{-4}	4.21×10^{-4}	82.74	4.00×10^{-4}	6.04×10^{-4}	68.39
Bromocresol Green	3.75×10^{-4}	5.42×10^{-4}	63.27	2.60×10^{-4}	4.02×10^{-4}	70.08

This means there is a reduction in electrical resistance and consequent increase in the transition of electrons in the material. **Table 2** shows the data obtained for electrical characterization, by Van der Pawn method, of the materials "PET + ITO + ZnONPs" before and after the deposition of the different dyes. The different dyes were tested in order to obtain data on the most efficient sensitizers for DSSC with the ZnO NPs thin films.

Since each dye has a difference in the absorption of the solar spectrum and, possibly, in the connection to the semiconductor layer. Occur that variations in the current values, DeltaV and sheet resistance depending on the dye used. The results, in ascending order, of the Sheet Resistance were: CR<AO<RC<BG.

Fig. 5 shows the sheet resistance ratio of films "PET+ITO+ZnONPs+Dye" versus open-circuit voltage (V_{oc}). The V_{oc} values were obtained after closing the cells and the application of iodine electrolyte, using a multimeter.
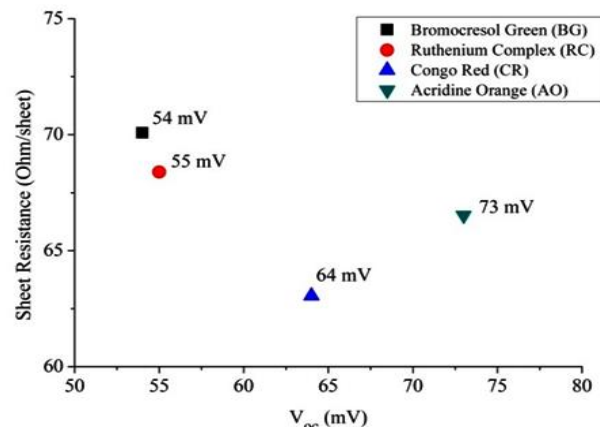

Fig. 5. Sheet resistance of the films "PET+ITO+ZnONPs+Dye" and open-circuit voltage (V_{oc}) after closing of the cells. Where V_{oc}= open-circuit voltage.

The lower sheet resistances were observed in the samples containing Congo Red and Acridine Orange dye films, 63.05 and 66.52 Ω/sheet, respectively. It is noted that the lower sheet resistance values obtained the best efficiency results in open-circuit voltage values (V_{oc}), i.e., higher efficiency transforming solar energy into electrical energy.

It is also important to mention that maximum absorption of the CR dyes surrounding 490 nm [**51,52**], having an E_g about 2.53 eV. We also note that the AO (monomer) dye has a maximum absorption around 492 nm, and consequently the E_g would be surrounding 2.52 eV [**53,54**]. Thus, it is assumed that the interaction between the substances that compose the solar cell were the best devices containing these dyes with smaller energy band gap, requiring less amount of solar energy for the movement of electrons between the layers of cells. Verifying higher energy conversion efficiency. Given these results, it is assumed that the encapsulation of cells with suitable material may obtain greater efficiency values of DSSCs.

Conclusion

In the present work, Pechini method was used for the synthesis of the ZnO NPs layer that was used in Grätzel solar cells with different dyes. This research presents results about sheet resistance of the ZnO nanoparticles and four different types of artificial dyes thin films. Also addresses the efficiency of photovoltaic devices, where we had their semiconductor layers of nanometric particles and their dyes deposited by spin-coating technique.

The produced ZnO NPs obtained a uniform crystal structure type Wurtzite, based on hexagonal tetragonal space group. The X-ray analysis showed a good crystallinity, free of secondary phases. Rietveld refinement analysis presented crystallites from 50 to 163 nm and an average diameter size of 115 nm. On the side of UV-Vis. analysis, the bandgap obtained for these nanoparticles was 3.39 eV, in accordance with literature.

With respect to the spin-coating technique, this showed to be suitable for preparing thin films of ZnO NPs and dyes. There was an increase of 11.15% between the lowest and highest sheet resistance of the parts containing dye films, i.e., comparing the Congo Red and Bromocresol Green thin films, respectively.

After closing the cells and applying iodine electrolyte, V_{oc} values were obtained using a multimeter. It is noted that the lower sheet resistance values obtained the best efficiency results in open-circuit voltage values, i.e., higher efficiency transforming solar energy into electrical energy. The best result was obtained with devices containing the dye Acridine Orange, with 73 mV of efficiency. Thus, the dye had the best result in optimizing the transport of charge carriers compared to other dyes. These absorb light radiation and assist in electron-hole exchange between the conductor and semiconductor materials system. Thus, this result suggests that the interaction between the layers was

satisfactory and the electrolyte penetrate through the pores of ZnO-dye layers, because among other factors there was an increase in the porosity and surface area of the NPs film.

Following the results, it was possible to compare the mounted devices efficiency with respect to the applied materials, such as ZnO nanoparticles with wurtzite type crystalline structure. It was observed that hybrid photovoltaic devices can be obtained with considerable efficiency and, high scientific and technological relevance for the generation of alternative energy to society. Future work can be carried out with specific encapsulation of the cells and in bench with illumination of a solar simulator.

In addition, it is very important to include the scientific community in every country at the international level in nanotechnology research with new materials, applied in the generation of alternative and clean energy.

Author's contributions

Conceived the plan: GVSL, WSH, PH; Performed the expeirments: GVSL, RCR, PHON, PH; Data analysis: GVSL, RCR, PHON; Wrote the paper: GVSL, WSH, PHON, LMB, PH. Authors have no competing financial interests.

Supporting information

Supporting informations are available from VBRI Press.

References

1. Hussein, A. K.; *Renew. Sustain. Energy Rev.*, **2015**, *42*, 460.
   DOI:10.1016/j.rser.2014.10.027
2. Dhankhar, M.; Pal Singh, O.; Singh, V. N.; *Renew. Sustain. Energy Rev.*, **2014**, *40*, 214.
   DOI:10.1016/j.rser.2014.07.163
3. Hosono, E.; Fujihara, S.; Honma, I.; Zhou, H.; *Adv. Mater.*, **2005**, *17*, 2091.
   DOI: 10.1002/adma.200500275
4. Choi, S. H.; Kim, E. G.; Park, J.; An, K.; Lee, N.; Kim, S. C.; Hyeon, T.; *J. Phys. Chem. B*, **2005**, *109*, 14792.
   DOI:10.1021/jp052934l
5. Wang, Z. L.; Wu, W.; *Angew. Chemie Int. Ed.*, **2012**, *51*, 11700.
   DOI:10.1002/anie.201201656
6. Cook, G.; Eber, K.; LaRocque, T.; *National Renewable Energy Laboratory - 2004 Research Review*; U. S., **2005**.
7. Zhang, L.; Yin, L.; Wang, C.; Lun, N.; Qi, Y.; Xiang, D.; *J. Phys. Chem. C*, **2010**, *114*, 9651.
   DOI:10.1021/jp101324a
8. Alias, S. S.; Mohamad, A. A.; *Synthesis of Zinc Oxide by Sol-Gel Method for Photoelectrochemical Cells*; Springer: Singapore Heidelberg New York Dordrecht London, **2014**.
   DOI:10.1007/978-981-4560-77-1
9. Barros, B. S.; Barbosa, R.; Santos, N. R.; Barros, T. S.; Souza, M. a.; *Inorg. Mater.*, **2006**, *42*, 1348.
   DOI:10.1134/S0020168506120119

10. He, G.; Cai, J. H.; Ni, G.; *Mater. Chem. Phys.*, **2008**, *110*, 110. **DOI:**10.1016/j.matchemphys.2008.01.023

11. Rautio, J.; Perämäki, P.; Honkamo, J.; Jantunen, H.; *Microchem. J.*, **2009**, *91*, 272. **DOI:**10.1016/j.microc.2008.12.007

12. Beek, W. J. E.; Wienk, M. M.; Kemerink, M.; Yang, X.; Janssen, R. a J.; *J. Phys. Chem. B*, **2005**, *109*, 9505. **DOI:**10.1021/jp050745x

13. Leprince-Wang, Y.; Yacoubi-Ouslim, a.; Wang, G. Y.; *Microelectronics J.*, **2005**, *36*, 625. **DOI:**10.1016/j.mejo.2005.04.033

14. Tang, Y.; Luo, L.; Chen, Z.; Jiang, Y.; Li, B.; Jia, Z.; Xu, L.; *Electrochem. commun.*, **2007**, *9*, 289. **DOI:**10.1016/j.elecom.2006.09.026

15. Wang, H.; Xie, C.; Zeng, D.; *J. Cryst. Growth*, **2005**, *277*, 372. **DOI:**10.1016/j.jcrysgro.2005.01.068

16. Zeng, H.; Cui, J.; Cao, B.; Gibson, U.; Bando, Y.; Golberg, D.; *Sci. Adv. Mater.*, **2010**, *2*, 336. **DOI:** 10.1166/sam.2010.1096

17. Izaki, M.; Watanabe, M.; Aritomo, H.; Yamaguchi, I.; Asahina, S.; Shinagawa, T.; Chigane, M.; Inaba, M.; Tasaka, A.; *Cryst. Growth Des.*, **2008**, *8*, 1418. **DOI:**10.1021/cg070164s

18. Guo, M.; Diao, P.; Wang, X.; Cai, S.; *J. Solid State Chem.*, **2005**, *178*, 3210. **DOI:**10.1016/j.jssc.2005.07.013

19. Sun, H.; Luo, M.; Weng, W.; Cheng, K.; Du, P.; Shen, G.; Han, G.; *Nanotechnology*, **2008**, *19*, 395602. **DOI:**10.1088/0957-4484/19/39/395602

20. Ma, T.; Guo, M.; Zhang, M.; Zhang, Y.; Wang, X.; *Nanotechnology*, **2007**, *18*, 35605. **DOI:**10.1088/0957-4484/18/3/035605

21. Chen, Y. J.; Zhu, C. L.; Xiao, G.; *Sensors Actuators, B Chem.*, **2008**, *129*, 639. **DOI:**10.1016/j.snb.2007.09.010

22. Meulenkamp, E. A.; *J. Phys. Chem. B*, **1998**, *102*, 5566. **DOI:**10.1021/jp980730h

23. Hu, Z.; Oskam, G.; Penn, R. L.; Pesika, N.; Searson, P. C.; *J. Phys. Chem. B*, **2003**, *107*, 3124. **DOI:**10.1021/jp020580h

24. Oskam, G.; *J. Sol-Gel Sci. Technol.*, **2006**, *37*, 161. **DOI:**10.1007/s10971-005-6621-2

25. Pechini, M. P.; Method of Preparing Lead and Alkaline Earth Titanates and Niobates and Coating Method Using the Same To Form a Capacitor, US3330697, **1967**.

26. Pereira, G. J.; Castro, R. H. R.; Hidalgo, P.; Gouvêa, D.; *Appl. Surf. Sci.*, **2002**, *195*, 277. **DOI:**10.1016/S0169-4332(02)00567-6

27. Castro, R. H.; Hidalgo, P.; Peres, H.; Fernandez, J. R.; Gouvêa, D.; *Sensors Actuators B Chem.*, **2008**, *133*, 263. **DOI:** 10.1016/j.snb.2008.02.021

28. R.S. Razavi; Loghman-Estarkib, M. R.; Farhadi-Khouzani, M.; *Acta Phys. Pol. A*, **2012**, *121*, 98. **DOI:**10.1007/s11671-009-9401-z

29. Gonçalves, A. de S.; Lima, S. A. M. de; Davolos, M. R.; *Eclética Química*, **2002**, *27*, 293. **DOI:** 10.1590/S0100-46702002000200025

30. Das, N. C.; Sokol, P. E.; *Renew. Energy*, **2010**, *35*, 2683. **DOI:**10.1016/j.renene.2010.04.014

31. Yap, C. K.; Tan, W. C.; Alias, S. S.; Mohamad, A. A.; *J. Alloys Compd.*, **2009**, *484*, 934. **DOI:**10.1016/j.jallcom.2009.05.073

32. O'Regan, B.; Grätzel, M.; *Nature*, **1991**, *353*, 737. **DOI:**10.1038/353737a0

33. Maçaira, J.; Andrade, L.; Mendes, A.; *Renew. Sustain. Energy Rev.*, **2013**, *27*, 334. **DOI:**10.1016/j.rser.2013.07.011

34. Karunakaran, C.; Jayabharathi, J.; Venkatesh Perumal, M.; Thanikachalam, V.; Kumar Thakur, P.; *J. Phys. Org. Chem.*, **2013**, *26*, 386. **DOI:**10.1002/poc.3100

35. Luz, G. V. S.; Roncoleta, R. C.; Santos, E. R.; Martins, M.; Hidalgo, P.; Hui, W. S.; In *XIII Brazilian MRS Meet.*; Brazilian MRS Meeting: João Pessoa: **2014** , p. 3.

36. Santos, E. R.; Luz, G. V. S.; Burini, E. C.; Takimoto, H. G.; Yoshida, S.; Vieira JR, H. R.; Falla, M. del P. H.; Hui, W. S.; In *XIV SLAP/ XII CIP 2014*; Brazilian Polymer Association ABPol: Porto de Galinhas/RN: **2014** , pp. 14–17.

37. Van der Pauw, L. J.; *Philips Res. Reports*, **1958**, *13*, 1.

38. Webster, J. G.; *The Measurement, Instrumentation and Sensors Handbook (Electrical Engineering Handbook)*; CRC Press: Davis/California, **1998**.

39. Grätzel, M.; *J. Photochem. Photobiol. C Photochem. Rev.*, **2003**, *4*, 145. **DOI:**10.1016/S1389-5567(03)00026-1

40. Rietveld, H. M.; *J. Appl. Crystallogr.*, **1969**, *2*, 65. **DOI:**10.1107/S0021889869006558

41. Rietveld, H. M.; *Acta Crystallogr.*, **1967**, *22*, 151. **DOI:**10.1107/S0365110X67000234

42. Lacerda, L. H. da S.; Lazaro, S. R. de; Ribeiro, R. A. P.; Oliveira, C. R. de; *An. do VII Work. Nanotecnologia Apl. ao Agronegócio*, **2013**, 425.

43. Kihara, K.; Donnay, G.; *Can. Mineral.*, **1985**, *23*, 647.

44. Dinnebier, R.; Friese, K.; In *Encycl. Life Support Syst.*; Ed.: P. Tropper(Eds.) Eolss Publishers: UK: **2003**.

45. Toby, B. H.; *Powder Diffr.*, **2006**, *21*, 67. **DOI:**10.1154/1.2179804

46. Feltrin, C. W.; Síntese E Propriedades Do ZnO: Correlaçao Entre Propriedades Estruturais E Atividade Fotocatalítica, Universidade Federal do Rio Grande do Sul, **2010**.

47. Bürger, T. S.; Desenvolvimento de Filmes de ZnO Para Aplicação Em Fotocatálise, Universidade Federal do Rio Grande do Sul, **2011**.

48. Murphy, A. B.; *J. Phys. D. Appl. Phys.*, **2006**, *39*, 3571. **DOI:**10.1088/0022-3727/39/16/008

49. Wang, Z. L.; *J. Phys. Condens. Matter*, **2004**, *16*, R829. **DOI:**10.1088/0953-8984/16/25/R01

50. Atkins, P. w.; Shriver, D. F.; *Química Inorgânica - 4ª Ed.*; Bookman, **2008**.

51. Klunk, W. E.; Jacob, R. F.; Mason, R. P.; *Quantifying Amyloid by Congo Red Spectral Shift Assay*; Elsevier, **1999**. **DOI:**10.1016/S0076-6879(99)09021-7

52. Ahsan, N.; Mishra, S.; Jain, M. K.; Surolia, A.; Gupta, S.; *Sci. Rep.*, **2015**, *5*, 9862. **DOI:**10.1038/srep09862

53. Fan, S.; Fischer, G.; Acridine Orange Derivatives and Their Use in the Quantitation of Reticulocytes in Whole Blood, US 5075556 A, **1991**.

54. Erik Droog; Tibbe, A.; Greve, J.; Gohel, D.; Terstappen, L.; Methods and Algorithms for Cell Enumeration in a Low-Cost Cytometer, WO 2003069421 A3, **2003**.